done essentially as in (3, 7).
7. M. Bafor, M. Smith, L. Jonsson, K. Stobart, S. Stymne, *Arch. Biochem. Biophys.* **303**, 145 (1993).
8. Monoclonal antibody to C_2A_5 was against P-450 reductase that was purified from *Helianthus tuberosus*.
9. F. J. van der Loo, P. Broun, S. Turner, C. Somerville, *Proc. Natl. Acad. Sci. U.S.A* **92**, 6743 (1995).
10. F. J. van de Loo, B. G. Fox, C. Somerville, in *Lipid Metabolism in Plants*, T. S. Moore, Ed. (CRC, Boca Raton, FL, 1993), pp. 91–126.
11. PCR primers for the Δ12 desaturase and castor Δ12 hydroxylase sequences were CAY GAR TGY GGN CAY CAY GC and CCN CKN ARC CAR TCC CAY TC, and for the Δ15 desaturase were ACN CAY CAY CAR AAY CAY GG and CAY TGY TTN CCN CKR TAC CA (N is A, G, C or T; R is A or G; Y is C or T; and K is G or T). The conditions used for PCR, at a concentration of 2.5 mM $MgCl_2$, were 94°C for 4 min, then 30 cycles of—94°C for 30 s, 50°C for 30 s, 72°C for 60 s—and finally one cycle of 72°C for 5 min.
12. Cotyledons from seeds harvested 17 to 20 days after flowering, were used to make a cDNA library with a Uni-ZAP XR cDNA cloning kit from Stratagene. After screening with a random primed probe, pBluescript phagemid was excised. This was used to create a double-stranded DNA plasmid.
13. Plasmid pVT-Crep1 was constructed by placing the insert from pCrep1 into the vector pVT100U, which contains the constitutive alcohol dehydrogenase promoter [T. Vernet, D. Dignard, D. Y. Thomas, *Gene* **52**, 225 (1987); R. Elble, *Biotechniques* **13**, 18 (1992)].
14. Yeast were grown in liquid medium without uracil at 28°C for 5 hours before linoleic acid and Tween 40 were added to a final concentration of 0.03% (w/v) and 1% (w/v), respectively. After a further 78 hours of cultivation, cells were washed and the lipids extracted. Methyl esters were prepared with 4% w/w methanolic HCl and analyzed by GLC with a glass column (2.5 m long with a 2-mm inner diameter) packed with 3% SP-2300 on Supelcoport 100/120 mesh (Supelco, Bellefonte, PA).
15. FADEA was prepared [R. Nilsson and C. Liljenberg, *Phytochem. Anal.* **2**, 253 (1991)] and injected directly for GLC-MS [Hewlett-Packard 5890 II GLC with a DB225 (J & W Scientific, Folsom, CA) in series with a Rtx 2330 (Restek, Bellefonte, PA) fused-silica capillary column coupled to a Hewlett-Packard 5989A mass spectrometer working in electron impact mode at 70 eV].
16. A binary vector for the acetylenase consisted of the Crep1 cDNA placed downstream of the −309 fragment from the napin promoter [K. Stålberg, M. Ellerström, L. Josefsson, L. Rask, *Plant Mol. Biol.* **23**, 671 (1993)] in the vector pGPTV-KAN [D. Becker, E. Kemper, J. Schell, R. Masterson, *ibid.* **20**, 1195 (1992)]. *Arabidopsis thaliana* Columbia (C-24) was transformed with *Agrobacterium tumefaciens* [D. Valvekens, M. Van Montagu, Van Lusbettens, *Proc. Natl. Acad. Sci. U.S.A.* **85**, 5536 (1988)].
17. Methyl esters were prepared by heating 10 to 30 whole seeds at 85°C for 90 min in 1 ml of 0.1 M sodium methoxide. Methyl esters were extracted with hexane and analyzed by GLC through a 50 m by 0.32 mm CP-Wax58-CB fused-silica column (Chrompack).
18. A *C. palaestina* library was prepared and screened as described (12).
19. The Cpal2 transformation was done as described (16) except that the binary vector used was pBI121 (Clonetech).
20. Diols were prepared from epoxy fatty acids purified from Cpal2-transformed *Arabidopsis*. They were converted further to trimethylsilyl ethers and analyzed by GLC-MS (15) with a DB23 fused-silica capillary column. The total ion chromatogram showed two peaks. The mass spectrum of the first eluting peak had prominent ions of mass 73, 172, 275, and 299. This indicated that the epoxy group was positioned at C-12 of a C_{18} fatty acid and that a double bond occurred between the epoxy group and the COOH-terminus. This mass spectra was identical to the spectra of a trimethylsilyl ether derivative of diols prepared from vernolic acid. The second peak had prominent ions of mass 73, 171, 273, and 299. This indicated the presence of two double bonds and an epoxy group positioned at C-12 in a C_{18} fatty acid.
21. N. Engeseth and S. Stymne, *Planta* **198**, 238 (1996).
22. P. Broun, N. Hawker, C. R. Somerville, in *Physiology, Biochemistry and Molecular Biology of Plant Lipids*, J. P. Williams, U. K. Mobashsher, N. W. Lem, Eds. (Kluwer Academic, Dordrecht, Netherlands, 1996), pp. 342–344.
23. J. Shanklin, E. Whittle, B. G. Fox, *Biochemistry* **33**, 12787 (1994).
24. J. Shanklin *et al.*, in (22), pp. 6–11.
25. J. Okuley *et al.*, *Plant Cell* **6**, 147 (1994).
26. J. Shanklin, J. Achim, H. Schmidt, B. G. Fox, E. Munck, *Proc. Natl. Acad. Sci. U.S.A.* **94**, 2981 (1997).
27. J. E. Colbert, A. G. Katapodis, S. W. May, *J. Am. Chem. Soc.* **112**, 3993 (1990).
28. L. Shu *et al.*, *Science* **275**, 515 (1997).
29. M. O. Bagby, M. Mikolajczak, K. L. Mikolajczak, *Alkali Isomerization of Crepenynic Acid to 8,10,12-Octadecatrienoic Acid.* U.S. patent no. 3,356,699 (1967).
30. European Molecular Biology Laboratory (EMBL) accession numbers are as follows: *C. palaestina* epoxygenase, Y16283; *C. alpina* acetylenase, Y16285; *C. palaestina* putative Δ12 desaturase, Y16284; *A. thaliana* Δ12 desaturase, L26296; and the castor bean oleate hydroxylase, U22378.
31. Pileup and Pretty, Wisconsin Package Version 9.0-UNIX, Genetics Computer Group, Madison, WI.
32. We thank A. Lesot, Instut de Biologie Moléculaire des Plantes, Strasbourg, France, for monoclonal antibody C_2A_5 to P-450 reductase and S. McKinney and A. T. Carter for technical assistance. Funded in part by the Swedish Foundation for Agricultural Research, the Swedish Natural Science Research Council, Stiftelsen Svensk Oljeväxtforskning, and European Union Grant number AIR2-CT94-0967.

18 December 1997; accepted 23 March 1998

A Role for the AKT1 Potassium Channel in Plant Nutrition

Rebecca E. Hirsch, Bryan D. Lewis, Edgar P. Spalding, Michael R. Sussman*

In plants, potassium serves an essential role as an osmoticum and charge carrier. Its uptake by roots occurs by poorly defined mechanisms. To determine the role of potassium channels in planta, we performed a reverse genetic screen and identified an *Arabidopsis thaliana* mutant in which the *AKT1* channel gene was disrupted. Roots of this mutant lacked inward-rectifying potassium channels and displayed reduced potassium (rubidium-86) uptake. Compared with wild type, mutant plants grew poorly on media with a potassium concentration of 100 micromolar or less. These results and membrane potential measurements suggest that the AKT1 channel mediates potassium uptake from solutions that contain as little as 10 micromolar potassium.

Potassium absorption by roots is essential for plant growth. Current models, which are elaborations of classic studies (1), state that K^+ absorption is mediated by cotransporters at micromolar K^+ concentrations and channels at higher concentrations (2–6). This notion is supported by the finding that plant genes encoding channels or cotransporters could complement yeast K^+-uptake mutants (6–8), but such experiments do not address which mechanisms are operating in the plant. Here we report an in planta genetic dissection of the role of the AKT1 channel in the uptake of K^+ by a root.

A transferred DNA (T-DNA) mutagenized population of *Arabidopsis* was screened for plants containing an insertional mutation in the root-specific K^+-channel gene *AKT1* by using the polymerase chain reaction (PCR)–based, reverse genetic method of Krysan *et al.* (9, 10). From a population of 14,200 different T-DNA lines, containing about 20,000 independent insertional events, we identified and isolated a single mutant plant (*akt1-1*) with a T-DNA insertion in *AKT1*. Southern blot analysis of the *akt1-1* locus (11) revealed a T-DNA insertion within the last exon of the coding region (Fig. 1). Sequence analysis reveals the T-DNA insertion site to be 4071 bases downstream of the start codon, and Northern blot analysis confirms that the mutation truncates the transcript by about 400 bases (12).

We examined the K^+ conductance of the plasma membrane in root cells, where high expression of *AKT1* was previously found (13). Microelectrodes inserted into cells approximately 150 μm from the apex of roots, which were bathed in 10 μM K^+ (14), revealed very negative resting membrane potentials (V_m) in both wild-type and *akt1-1* seedlings (Fig. 2B). A 10-fold increase in the extracellular K^+ concentra-

R. E. Hirsch, Department of Horticulture and Program in Cellular and Molecular Biology, University of Wisconsin, Madison, WI 53706, USA.
B. D. Lewis, Department of Botany, University of Wisconsin, Madison, WI 53706, USA.
E. P. Spalding, Department of Botany and Program in Cellular and Molecular Biology, University of Wisconsin, Madison, WI 53706, USA.
M. R. Sussman, Biotechnology Center, Department of Horticulture and Program in Cellular and Molecular Biology, University of Wisconsin, Madison, WI 53706, USA.

*To whom correspondence should be addressed.

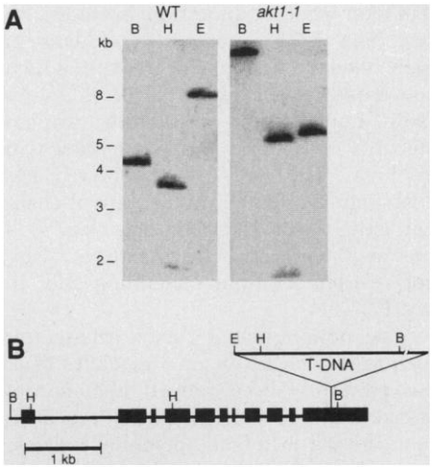

Fig. 1. Analysis of the *AKT1* gene. (**A**) Southern blot analysis of genomic DNA digested with Bam HI (lanes B), Hind III (lanes H), or Eco RI (lanes E) and hybridized with radiolabeled DNA corresponding to the *AKT1* coding region. (**B**) Restriction map of *AKT1* genomic DNA based on Southern analysis (A) and sequence analysis (*12*). Large and small boxes represent exons and introns, respectively. Structure of the T-DNA insertion 3′ to the Bam HI site is undefined. T-DNA is not drawn to scale.

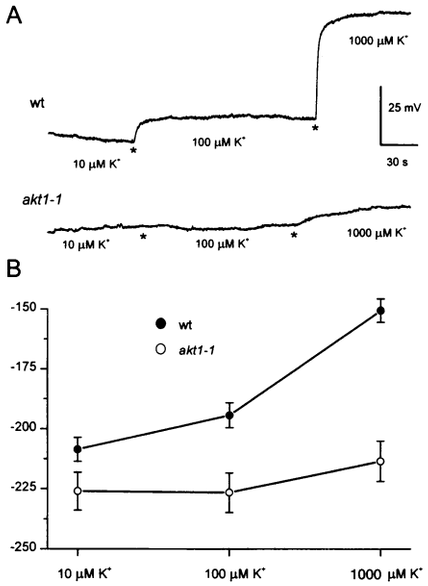

Fig. 2. Membrane potential (V_m) in apical root cells. (**A**) Representative recordings of shifts in V_m in response to the indicated changes in extracellular [K^+] indicated a significant K^+ permeability of the wild-type plasma membrane. The much smaller shifts in *akt1-1* roots indicate that the K^+ permeability was greatly reduced by the mutation. (**B**) The average steady-state V_m in millivolts (ordinate) obtained at each extracellular [K^+] (n = 10 for both wild type and *akt1-1*). Qualitatively similar results were obtained in 25 additional experiments that are not included here because of slight differences in the ionic conditions used.

tion significantly depolarized the membrane in wild-type roots but had no effect on V_m in *akt1-1* seedlings (Fig. 2). These results indicate that AKT1 is responsible for the K^+ permeability of these apical root cells. Also, using 80 mM as the cytoplasmic K^+ concentration (*4*, *15*) in the Nernst equation, it follows that a V_m of at least −230 mV is required for K^+ uptake to occur passively through a channel. Twenty percent of wild-type cells met this condition without making corrections for the fact that intracellular microelectrodes underestimate V_m (*16*). Our results indicate that in wild-type seedlings passive uptake of K^+ by AKT1 could occur from extracellular solutions as dilute as 10 μM.

Whole-cell recording from wild-type root protoplasts (Fig. 3A) showed that voltage steps from −10 mV to positive membrane potentials elicited outward, time-dependent currents (*17*). Steps to negative voltages always elicited inward currents that in some cells were largely time dependent and in others were only partly so. Evidence that the inward currents in Fig. 3A were carried by K^+ was obtained by the use of largely impermeant anions in the patch pipette, by their disappearance when extracellular K^+ was replaced by Cs^+ (*18*), and by the analysis of tail currents shown in Fig. 3B (*19*). The current-voltage (*I-V*) relationship for the tail currents reversed within 5 mV of the theoretical value for a K^+-selective channel exposed to a threefold K^+ gradient (E_K = −27 mV) (Fig. 3B). Individual 16 pS K^+-selective channels in patches of membrane excised from wild-type protoplasts (Fig. 3C) displayed a voltage dependence and activation threshold consistent with their being responsible for the inward currents (Fig. 3, A and B) and the resting K^+ permeability determined in planta (Fig. 2).

Consistent with the data in Fig. 2, patch-clamp recordings of *akt1-1* root cells revealed no inward currents, although the outward currents were normal (Fig. 3D).

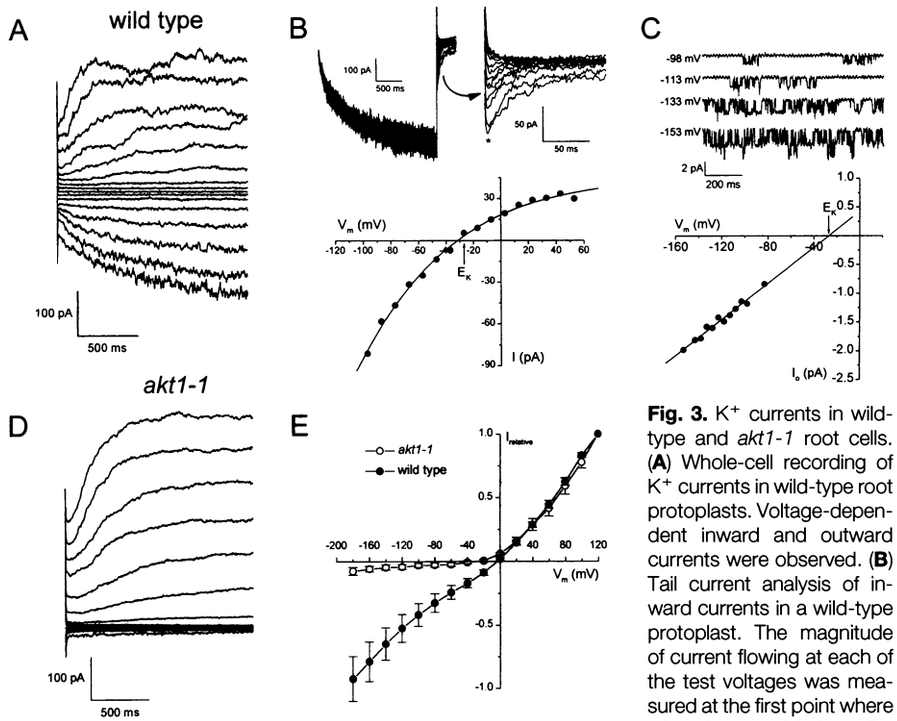

Fig. 3. K^+ currents in wild-type and *akt1-1* root cells. (**A**) Whole-cell recording of K^+ currents in wild-type root protoplasts. Voltage-dependent inward and outward currents were observed. (**B**) Tail current analysis of inward currents in a wild-type protoplast. The magnitude of current flowing at each of the test voltages was measured at the first point where relaxation could be discerned (asterisk) and was plotted versus the test voltage to construct the *I-V* curve shown. The close agreement between the zero-current voltage (reversal potential) of the *I-V* curve and the equilibrium potential for K^+ (E_K) indicates that the inward-rectifying currents were carried by K^+. The experiment shown is representative of three independent trials. (**C**) Single K^+ channels in outside-out patches of plasma membrane excised from wild-type root cells. Open-channel current amplitudes were measured and plotted versus the clamped voltage to construct the *I-V* curve. The close agreement between the reversal potential and E_K indicates that the inward-rectifying currents were carried by K^+. The currents were low-pass filtered at 0.5 kHz and digitized at 1 kHz. (**D**) Whole-cell recording of K^+ currents in *akt1-1* root protoplasts. Inward currents were absent but outward currents were the same as in wild-type root protoplasts. (**E**) Steady-state, whole-cell *I-V* curves reveal the absence of inward currents in *akt1-1*. The raw currents were normalized relative to the value at +120 mV, averaged (n = 10 for wild type and 6 for *akt1-1*), and plotted versus the clamp potential. No leak subtraction or other manipulation of the currents was performed. In (A), (D), and (E), voltage steps ranged from +120 to −180 mV in 20-mV increments.

The normalized steady-state *I-V* relationships shown in Fig. 3E illustrate that the *akt1-1* mutation selectively abolished the inward component of the K^+ conductance of the membrane. From the electrophysiological results presented in Figs. 2 and 3, we conclude that *AKT1* encodes the inward-rectifying channel responsible for the resting K^+ permeability of cells in the root apex.

Growth of *akt1-1* plants on many nutrient media was indistinguishable from that of wild type. However, growth of *akt1-1* plants on media containing ≤100 μM K^+ (*20*) was significantly inhibited compared with wild type in the presence of NH_4^+ (Fig. 4, A and B). At 10 μM, most *akt1-1* seeds failed to fully emerge from the seed coat (Fig. 4A), but they resumed normal growth after transplantation to media with high K^+ concentration (*12*). Growth of *akt1-1* seedlings on 1 mM K^+ was only slightly reduced relative to wild type (Fig. 4, A and B).

To determine whether the T-DNA insertion cosegregated with the mutant phenotype, we crossed homozygous *akt1-1* plants to wild-type *Arabidopsis* of the same ecotype (WS). Self-crossed F_2 seedlings were grown as described (*20*). The wild-type (normal growth) or mutant (poor growth) phenotype segregated as a single, recessive gene (*21*). For cosegregation analysis, the genotype of segregating F_2 plants was analyzed by PCR using *AKT1*- (*10*) and T-DNA-specific primers (*9*). Twenty of 21 homozygous *akt1-1* plants grew poorly, and 31 of 36 plants that were heterozygous or homozygous wild type grew normally. Several homozygous wild-type and homozygous mutant F_2 plants were self-crossed; phenotypic analysis demonstrated that >90% of the progeny from the *akt1-1* homozygous parents were phenotypically mutant, and 90% of the progeny from wild-type parents were phenotypically wild type. This analysis demonstrates that the mutant phenotype shows >90% penetrance and is genetically linked to the *akt1-1* locus.

To determine the effect of the *akt1-1* mutation on K^+ absorption by roots, we performed $^{86}Rb^+$ tracer flux analysis in roots obtained from plants grown in a high concentration of external K^+ (*22*). Uptake rates from media containing various amounts of K^+ and NH_4^+ are shown in Table 1. The *akt1-1* roots showed less $^{86}Rb^+$ uptake than wild type. Loss of channel activity in *akt1-1* root cells (Fig. 3) is thus associated with reduced rates of $^{86}Rb^+$ uptake from solutions containing only 10 μM Rb^+.

The notion that a passive transporter such as the AKT1 channel mediates what has previously been termed high-affinity uptake has been suggested (*23*). Our measurements of membrane potential indicate that it is energetically feasible in the root cells studied here. Dependence of the *akt1-1* growth phenotype on NH_4^+ suggests that this cation inhibits parallel, non-AKT1 K^+ uptake pathways, making growth dependent on AKT1. This is consistent with our observation as well as that of others that NH_4^+ inhibited $^{86}Rb^+$ uptake in wild-type roots (*12, 24*). As reverse genetic strategies identify plants with disruptions in other K^+ transporters, analyses of double and triple mutant combinations will directly test this hypothesis.

Table 1. Radioactive tracer flux analysis of Rb^+ uptake in *akt1-1* and wild-type roots. The uptake solution (*22*) contained Rb(^{86}Rb)Cl at the concentrations indicated. Each value is the mean rate of uptake (n = 4) ± SEM.

	10 μM RbCl (nanomoles per gram fresh weight per hour)	100 μM RbCl (nanomoles per gram fresh weight per hour)	1 mM RbCl (nanomoles per gram fresh weight per hour)
Wild type	44.8 ± 7.6	112.1 ± 24.8	282.8 ± 44.1
akt1-1	3.1 ± 0.3	23.3 ± 1.3	145.9 ± 10.1

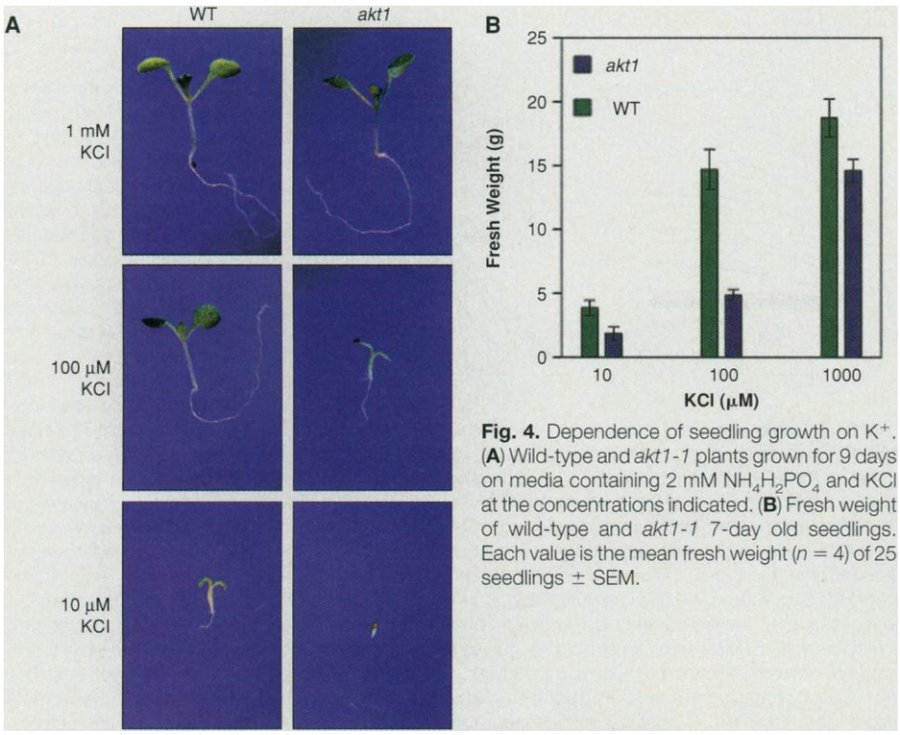

Fig. 4. Dependence of seedling growth on K^+. (**A**) Wild-type and *akt1-1* plants grown for 9 days on media containing 2 mM $NH_4H_2PO_4$ and KCl at the concentrations indicated. (**B**) Fresh weight of wild-type and *akt1-1* 7-day old seedlings. Each value is the mean fresh weight (n = 4) of 25 seedlings ± SEM.

REFERENCES AND NOTES

1. E. Epstein, D. W. Rains, O. E. Elzam, *Proc. Natl. Acad. Sci. U.S.A.* **49**, 684 (1963).
2. L. V. Kochian and W. J. Lucas, *Plant Physiol.* **70**, 1723 (1982); L. V. Kochian, J. Xin-zhi, W. J. Lucas, *ibid.* **79**, 771 (1985); S. K. Roberts and M. Tester, *Plant J.* **8**, 811 (1995); J. I. Schroeder and H. H. Fang, *Proc. Natl. Acad. Sci. U.S.A.* **88**, 11583 (1991).
3. F. J. M. Maathuis and D. Sanders, *Proc. Natl. Acad. Sci. U.S.A.* **91**, 9272 (1994).
4. F. J. M. Maathuis and D. Sanders, *Planta* **191**, 302 (1993).
5. F. J. M. Maathuis and D. Sanders, *ibid.* **197**, 456 (1995).
6. D. P. Schachtman and J. I. Schroeder, *Nature* **370**, 655 (1994).
7. J. A. Anderson, S. S. Huprikar, L. V. Kochian, W. J. Lucas, R. F. Gaber, *Proc. Natl. Acad. Sci. U.S.A.* **89**, 3736 (1992).
8. H. Sentenac *et al.*, *Science* **256**, 663 (1992).
9. P. J. Krysan, J. C. Young, F. Tax, M. R. Sussman, *Proc. Natl. Acad. Sci. U.S.A.* **93**, 8145 (1996).
10. *AKT1*-specific primers used were 5'- GCTGCTTATTTTGCCTCTTTTGCCGAAAC-3' and 5'-ACCCAATTCTAGCAACTCCTTGAAACTCC-3'.
11. Genomic DNA from *akt1-1* and wild-type seedlings (ecotype WS) was digested with the restriction enzymes indicated, separated on an agarose gel, transferred to nylon membrane (Magnagraph from MSI), and hybridized to a ^{32}P-labeled probe corresponding to 4.3 kb of wild-type *AKT1* genomic DNA. Radioactivity bound to blots was measured with a PhosphorImager (Molecular Dynamics).
12. R. E. Hirsch, data not shown.
13. D. Lagarde *et al.*, *Plant J.* **9**, 195 (1996).
14. Wild-type and *akt1-1* seeds were grown vertically on agar plates containing 100 μM K^+ (*20*) for 4 to 9 days, lifted from the agar, and mounted horizontally in a recording chamber containing the growth medium without agar. After 1 hour of recovery, the membrane potential of a root cell was measured with a 1 M KCl microelectrode and an Ag/AgCl reference

electrode in the flowing bath solution, which were connected to a GeneClamp 500 amplifier (Axon Instruments, Foster City, CA) interfaced with a computer. A drop of water at 0°C, which was added to the recording chamber at the end of each experiment, produced the expected large depolarization mediated by Ca^{2+} and Cl^- channels [B. D. Lewis, C. Karlin-Neumann, R. W. Davis, E. P. Spalding, *Plant Physiol.* **114**, 1327 (1997)], a test of proper cell impalement.

15. D. J. Walker, R. A. Leigh, A. J. Miller, *Proc. Natl. Acad. Sci. U.S.A.* **93**, 10510 (1996).
16. The shunt resistance between an inserted electrode and the membrane permits a depolarizing current to flow [T. H. Goldsmith and M. H. M. Goldsmith, *Planta* **143**, 267 (1978)], the effect of which may be to underestimate V_m by 20 to 50 mV [W. Gassmann and J. I. Schroeder, *Plant Physiol.* **105**, 1399 (1994)]. Corrections of that magnitude would shift each of our V_m measurements, the most positive of which was −193 mV, to values more negative than −230 mV.
17. Plants were grown vertically on Petri plates containing 1.5% (w/v) agar, 1 mM KCl, and 1 mM $CaCl_2$ in continuous light for 4 to 5 days. Root protoplasts were prepared by cutting the root about 150 μm from the tip with a micromanipulator-mounted razor. The cut seedlings were infiltrated with an enzyme solution containing Cellulysin (12 mg/ml) (Calbiochem), Pectinase (2 mg/ml) (Sigma), and bovine serum albumin (5 mg/ml) (Sigma) dissolved in 10 mM KCl, 1 mM $CaCl_2$, 5 mM MES, and 300 mM sorbitol {pH 5.2 with 1,3-bis[tris(hydroxymethyl)methylamino]propane (BTP)} using a vacuum produced by a faucet aspirator. After 2 hours of incubation, the seedlings were rinsed in the solution without enzymes and stored at 4°C or placed in a 500- μl recording chamber containing 10 mM $CaCl_2$, 30 mM KCl, 5 mM Hepes, and 120 to180 mM sorbitol (pH 7.0 with BTP). Protoplasts of nonepidermal cells emerged from the cut end of the otherwise undigested root. Patch pipettes were filled with 130 mM K-glutamate, 2 mM EGTA, 5 mM Hepes, and 4 mM Mg–adenosine triphosphate (Mg-ATP) (pH 7.0 with BTP). Patch-clamp equipment and procedures were as described [M. H. Cho and E. P. Spalding *Proc. Natl. Acad. Sci. U.S.A.* **93**, 8134 (1996)]. Our procedures led to observations of inward currents in all patch-clamped wild-type cells. Lower percentages reported by others (*5*) may be explained by different growth conditions, different voltage protocols, or use of different tissue. We encountered more variability in the voltage dependence of the inward currents than has been reported for heterologously expressed inward rectifiers [F. Gaymard *et al.*, *J. Biol. Chem.* **271**, 22863 (1996)]. This variability is responsible for the appearance of weak rectification in the averaged whole-cell *I-V* curve in Fig. 3E. Channel gating may have been affected by cytoplasmic components that washed out in some patch-clamped protoplasts.
18. B. D. Lewis and E. P. Spalding, data not shown.
19. Patch pipettes were filled with 390 mM K-glutamate, 2 mM EGTA, 5 mM Hepes, and 4 mM Mg-ATP (pH 7.0 with BTP). The bath contained 130 mM KCl, 10 mM $CaCl_2$, and 5 mM Hepes (pH 7.0 with BTP). Tail currents were evoked by clamping V_m at −200 mV before stepping to a series of more positive potentials.
20. Plants were grown in continuous light on media containing KCl at the concentrations indicated plus 0.8% (w/v) agarose (Bio-Rad, Hercules, CA), 0.5% (w/v) sucrose, 2.5 mM $NaNO_3$, 2.5 mM $CaNO_3$, 2 mM $NH_4H_2PO_4$, 2 mM $MgSO_4$, 0.1 mM FeNaEDTA, 25 μM $CaCl_2$, 25 μM H_3BO_3, 2 μM $ZnSO_4$, 2 μM $MnSO_4$, 0.5 μM $CuSO_4$, 0.2 μM Na_2MoO_4, and 0.01 μM $CoCl_2$, adjusted to pH 5.7 with NaOH.
21. Of 104 seedlings tested, 23 were phenotypically scored as mutant and 88 were scored as wild type, giving $x^2 = 0.346$ (based on the expected ratio of three wild type to one mutant); $P > 0.05$.
22. Wild-type and *akt1-1* plants were grown on agar containing MS salts and 5% (w/v) sucrose in constant light for 14 days. Roots were excised, weighed, and washed for 16 to 17 hours in a K^+-free desorption solution (DS) containing 1.5 mM $CaCl_2$ adjusted to pH 5.7 with CaOH. Roots were incubated for 10 min in DS containing 4 mM NH_4Cl and 10 μM, 100 μM, or 1 mM $Rb(^{86}Rb)Cl$ and then washed two times for 10 min each in ice-cold DS. Radioactivity was measured by detection of Cerenkov radiation.
23. J. I. Schroeder, J. M. Ward, W. Gassmann, *Annu. Rev. Biophys. Biomol. Struct.* **23**, 441 (1994); W. Gassmann, J. M. Ward, J. I. Schroeder, *Plant Cell* **5**, 1491 (1993).
24. Y. Cao, A. D. M. Glass, N. M. Crawford, *Plant Physiol.* **102**, 983 (1993); F. R. Vale, W. A. Jackson, R. J. Volk, *ibid.* **84**, 1416 (1987); F. R. Vale, R. J. Volk, W. A. Jackson, *Planta* **173**, 424 (1988).
25. Supported by the Department of Energy (DOE)/NSF/USDA Collaborative Research in Plant Biology Program (BIR-9220331), funds to R.E.H. from the NIH University of Wisconsin Cellular and Molecular Biology Training Grant (GM07215), to M.R.S. from DOE (DE-FG02-88ER13938) and NSF (DCB-90-04068), and to E.P.S. from the NASA/NSF Network for Research on Plant Sensory Systems (IBN-9416016). We thank T. Janczewski and R. Meister for technical assistance and P. Krysan, W. Robertson, J. Satterlee, and J. Young for helpful comments on the manuscript.

26 November 1997; accepted 27 March 1998

Knowing Where and Getting There: A Human Navigation Network

Eleanor A. Maguire,* Neil Burgess, James G. Donnett, Richard S. J. Frackowiak, Christopher D. Frith, John O'Keefe

The neural basis of navigation by humans was investigated with functional neuroimaging of brain activity during navigation in a familiar, yet complex virtual reality town. Activation of the right hippocampus was strongly associated with knowing accurately where places were located and navigating accurately between them. Getting to those places quickly was strongly associated with activation of the right caudate nucleus. These two right-side brain structures function in the context of associated activity in right inferior parietal and bilateral medial parietal regions that support egocentric movement through the virtual town, and activity in other left-side regions (hippocampus, frontal cortex) probably involved in nonspatial aspects of navigation. These findings outline a network of brain areas that support navigation in humans and link the functions of these regions to physiological observations in other mammals.

Where am I? Where are other places in the environment? How do I get there? Questions such as these reflect the essential functions of a navigation system. The neural basis of way-finding activity has been extensively studied. Spatially tuned neurons found in the hippocampal formation of freely moving rats [place cells coding for the rat's location (*1*) and head direction cells coding for its orientation (*2*)] support the idea that this part of the brain provides an allocentric (world-centered) representation of locations, or cognitive map (*3*). The posterior parietal lobe has been implicated in providing complementary egocentric representations of locations (centered on parts of the body) (*4*). Other brain regions, such as the dorsal striatum (*5*), have also been identified as possible elements of a navigation system. In humans, there has been much evidence for the involvement of the hippocampus in episodic memory, the memory for events set in their spatio-temporal context (*3*, *6*). By contrast, the role of the hippocampus in human navigation has remained controversial, and the wider neural network supporting human navigation is even less well understood. We attack this issue by combining functional neuroimaging with a quantitative characterization of human navigation within a complex virtual reality environment.

We used positron emission tomography (PET) (*7*) to scan subjects while they navigated to locations in a familiar virtual reality town using their internal representation of the town built up during a continuous period of exploration immediately before scanning (Fig. 1A). In one navigation condition, the subjects could head directly toward the goal (nav1), while in the other (nav2), direct routes were precluded by closing some of the doors and placing a barrier to block one of the roads, forcing the subjects to take detours. Navigation was compared to a task in which subjects moved through the town following a trail of arrows, thus not needing to refer to an internal representation of the town. An additional task requiring the identification of features in static scenes from the town was included for contrast with the three dynamic tasks (*8*).

We first investigated which brain regions were involved in successful naviga-

E. A. Maguire, R. S. J. Frackowiak, C. D. Frith, Wellcome Department of Cognitive Neurology, Institute of Neurology, University College London, 12 Queen Square, London WC1N 3BG, UK.
N. Burgess, J. G. Donnett, J. O'Keefe, Department of Anatomy and Developmental Biology and Institute of Cognitive Neuroscience, University College London, Gower Street, London WC1E 6BT, UK.

*To whom correspondence should be addressed. E-mail: e.maguire@fil.ion.ucl.ac.uk